Article published online: 2024-12-06

Original Article

Automated Assessment of Sarcopenia with Hounsfield Unit Average Calculation in Computed Tomography Scans Using Deep Learning Techniques

Vinayak Rengan[1] Pravin Meenashi Sundaram[2] Eham Arora[3] Rengan Ravanasamudram Sitaraman[4] Praveen Sekaran[5] Rohit Kalla[6] Ashvind Bawa[7] Naveen Alexander[8] Rochita V. Ramanan[9]

[1] Department of Pediatric Surgery, SMS Medical College, Jaipur, Rajasthan, India
[2] Department of Renal Transplant Surgery, Sheffield Teaching Hospitals NHS Foundation Trust, Sheffield, United Kingdom
[3] Department of General Surgery, Grant Medical College & Sir JJ Group of Hospitals, Mumbai, Maharashtra, India
[4] Department of General Surgery, Chennai Hernia Center, Chennai, Tamil Nadu, India
[5] Department of General Surgery, Basildon and Thurrock University Hospital, Mid and South Essex NHS Foundation Trust, Basildon, Nether Mayne, United Kingdom
[6] Department of Research Science, Curium Life Tech, Chennai, Tamil Nadu, India
[7] Department of Surgery, Dayanand Medical College and Hospital, Ludhiana, Punjab, India
[8] Department of General Surgery, Sri Ramachandra Institute of Higher Education and Research, Chennai, Tamil Nadu, India
[9] Department of Radiology, Advantage Imaging and Research Institute, Chennai, Tamil Nadu, India

Address for correspondence Pravin Meenashi Sundaram, MS, DNB, MRCS, Q5 Room 18, Q5Q6 Accommodation Block, Sheffield Teaching Hospitals, Norwood Grange Drive, Sheffield S57AU, United Kingdom (e-mail: bean.sundar@gmail.com).

J Gastrointestinal Abdominal Radiol ISGAR

Abstract

Introduction Skeletal muscle is increasingly plastic with an ability to gain or lose tissue. Depletion of muscle mass and quality occurs due to various factors such as aging, disease, and disuse. Sarcopenia can be loosely defined as a significant loss of muscle mass and function. Sarcopenia is now recognized as an independent risk factor for various patient-related negative outcomes after various surgeries. Various computed tomography (CT) based imaging indices for assessment of sarcopenia exist in practice. The psoas muscle Hounsfield unit average calculation (HUAC) has been proven to be an effective one as it is independent of patient anthropometric data, and it can be calculated in the images provided.

Aim The aim of this study is to develop automated tools for estimation of the HUAC using deep learning algorithms.

Materials and Methods A total of 41 abdominal CTs were used. Ground truth was established and validated by two radiologists with more than 5 and 10 years of experience each. Models were trained to identify the psoas muscle among the slices and calculate the HUAC.

Results At inference, an average intersection over union (IoU) value of 90% was obtained between the deep learning model outputs and the original annotated test

Keywords
- deep learning
- HUAC
- muscle quality
- sarcopenia

DOI https://doi.org/10.1055/s-0044-1795111.
ISSN 2581-9933.

Thieme Medical and Scientific Publishers Pvt. Ltd., A-12, 2nd Floor, Sector 2, Noida-201301 UP, India

images for the CT slices. The Dice coefficient was 0.90 between the ground truth labels and the output from the model.

Conclusion We have demonstrated the accuracy of our deep learning–based algorithm for quantifying the psoas muscle HUAC, which is a marker for sarcopenia. There is a potential for a fully automated measure to calculate the HUAC for any patient undergoing CT scan.

Introduction

Sarcopenia is a progressive and generalized skeletal muscle disorder that is associated with increased likelihood of adverse outcomes.[1] It is characterized by the gradual loss of skeletal muscle mass, strength, and function. It has emerged as a significant public health concern recently due to its impact on and relationship with disability, falls, osteoporosis, prolonged hospital stays, higher postoperative complications, readmission rates, and perioperative mortality.[2–5] Despite its major impact on patient outcomes, the loss of tissue often goes unrecognized due to its gradual decline.[6]

There exist multiple ways and criteria to define sarcopenia, which include imaging and nonimaging techniques. Questionnaires such as the SARC-F scale (slowness, assistance walking, rising from the chair, climbing stairs, and falls)[7] are used in certain centers, but these have moderate predictive value.[6] Physical performance assessment and strength assessment using gait speed, chair rise time, balance test, and dynamometer testing are also used. Anthropometric measurements used to assess sarcopenia include body mass index (BMI), skin fold thickness, and bioelectrical impedance testing. However, the real challenge with nonimaging modalities is the lack of accuracy and poor correlation with patient outcomes. Furthermore, orthopaedic disorders, neurological conditions, and medications may also lead to false positives.[6]

Imaging has therefore emerged as the default assessment tool for sarcopenia in recent times. Imaging parameters include dual energy X-ray absorptiometry (DEXA), sonography, echo intensity, computed tomography (CT) scans and magnetic resonance imaging (MRI). In this article, we focus on CT scans as they are the most employed form of imaging before major abdominal surgery and lend themselves to accurate sarcopenia assessment.

Several CT-based indices for sarcopenia exist. The ones utilizing muscle volumes are not in vogue due to the time and effort investment needed for volumetric calculations. Various CT-assessed sarcopenia indices have been reported in the literature, which include skeletal muscle index/total abdominal muscle area, simple moving average/body surface area index, psoas muscle index/total psoas muscle area, muscle attenuation/radiation attenuation, intramuscular adipose tissue content, Hounsfield unit average calculation (HUAC), lean psoas muscle area, and total psoas muscle volume.[8]

HUAC has emerged as an efficient index for sarcopenia assessment as it is independent of the patient's anthropometric data, can be calculated exclusively from CT images, and does not need contrast administration. A person is labeled sarcopenic if his or her HUAC lies within the lowest gender-specific quartile.[9]

Given the objective nature of the scoring systems and their reliance on accurate image interpretation, there exists an opportunity to automate the calculation. The recent emergence of deep learning using convolutional neural networks in areas such as image recognition, classification, and segmentation can potentially make this exercise attainable and more objective.[8]

In pursuit of improved accuracy and efficiency, which may help make sarcopenia scoring available to a broader section of the patient population, our study endeavors to harness deep learning technology, resulting in the development of a robust model that can calculate HUAC directly from CT images.

Materials and Methods

Our tool for sarcopenia detection is a part of a broader deep learning model (DLM) that was developed for abdominal wall assessment in the hernia subspecialty. Data included CT scans with normal findings and abdominal wall hernias, which were obtained after internal review board approvals at two centers: Madras Medical College, Chennai, India, and Grant Medical College, Mumbai, India. The study was Health Insurance Portability and Accountability Act of 1996 (HIPAA) compliant and adhered to protocols set by National Ethical Guidelines for Biomedical and Health Research involving Human Participants, Indian Council for Medical Research (ICMR), 2017.[10] The ethics board of the institution waived the need for individual patient consents as per the ICMR guidelines.

In this retrospective study, we employed previously conducted imaging studies for system testing and analysis, rendering the need for informed consent waived. All scans were anonymized at source prior to inclusion within the study to ensure HIPAA compliance. These scans spanned a duration of 13 months from November 2021 to December 2022. Forty-one CT scans of the abdomen were randomly selected and retrieved through the Picture Archiving and Communication System (PACS) at the centers. We excluded scans with lumbar metallic implants

that caused substantial artifacts affecting the visualization and segmentation of the psoas muscles. No disease pathology was excluded from the study. This approach ensures the accuracy of sarcopenia measurements and minimizes the impact of artifacts on the model's performance.

CT Scanning Protocol

The deep learning algorithm for sarcopenia assessment was trained on plain abdominal CT scans. Supine position breath-hold CT acquisitions of the abdomen and pelvis were performed without intravenous (IV) contrast in multidetector 8- to 64-slice CT scanners. To ensure proper segmentation of a diverse range of CT images, the algorithm was designed to accommodate a wide range of tube currents and slice thicknesses, producing significant variations.

A brief overview of the data acquisition and preprocessing is provided in ►**Fig. 1**.

Generation of Ground Truth Labels

Ground truth is crucial in training deep learning algorithms, and it serves to feed accurate and reliable reference data, allowing the algorithm to learn from correct examples and improve its performance. In other words, it serves as a benchmark against which the algorithm's predictions are compared, promoting its adjustments toward higher accuracy. The forty-one CTs were processed to lower image resolution, that is, 128×128 pixels and min-max normalized them. Binary masked images were generated with left and right psoas muscles assigned label 1 and background as 0. Axial images of every slice including L2–L4 vertebrae were extracted from the CTs and used for analysis. Ground truth segmentation maps were created using open-source ITK-SNAP ver3.8 software.[11] Ground truth labels were defined using the segmentation maps of the psoas muscles created by manual annotation on CTs by a radiologist (with >5 years of clinical experience). These were further verified by

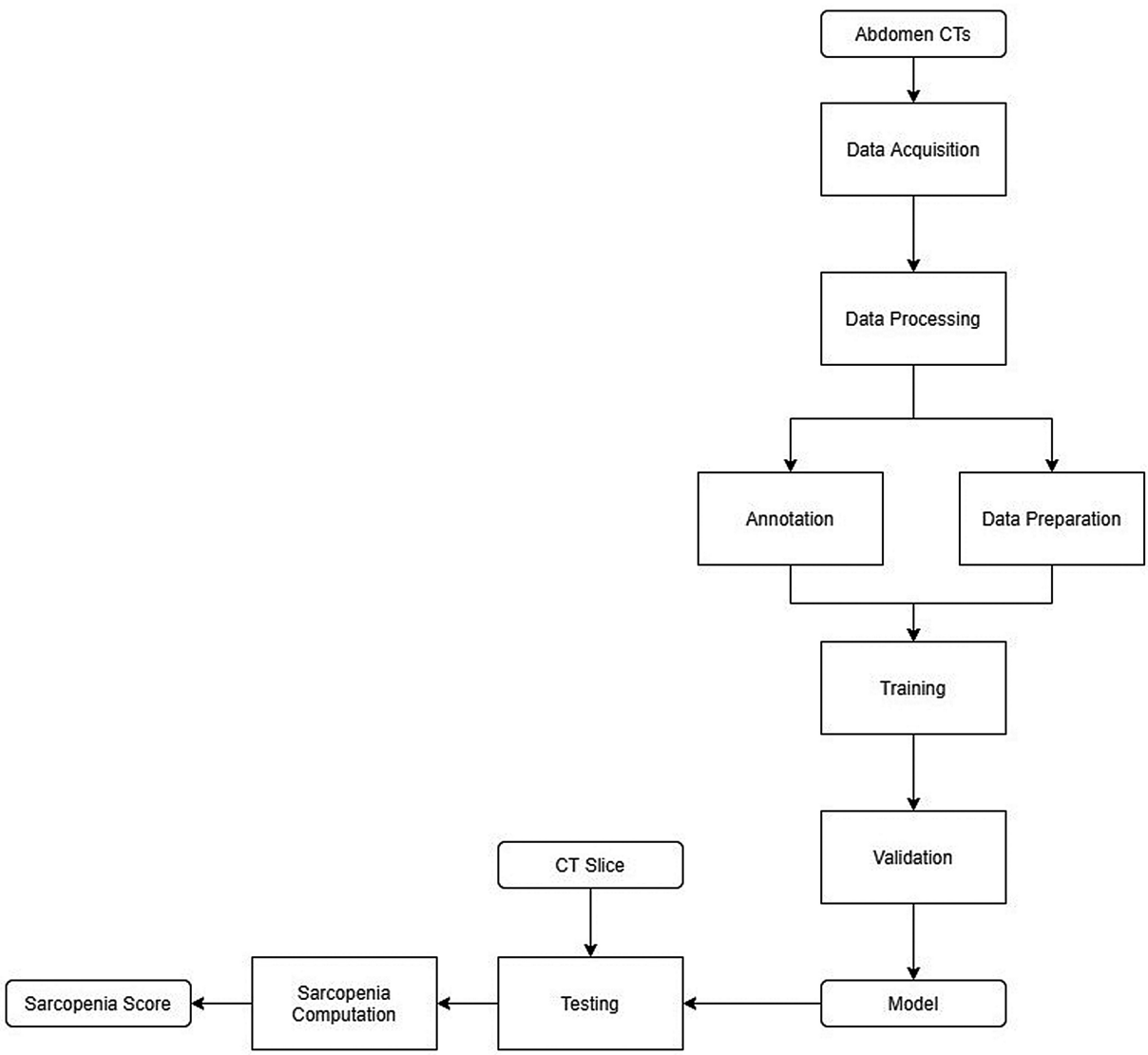

Fig. 1 Sarcopenia calculation data workflow. CT, computed tomography.

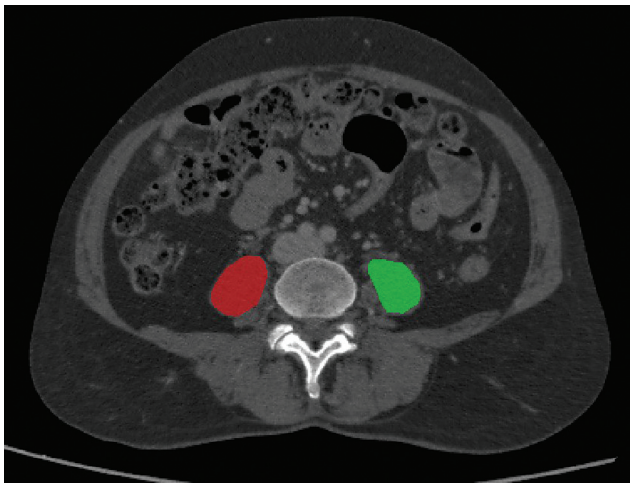

Fig. 2 Ground truth labels of the psoas major muscle.

another seasoned radiologist (>10 years of clinical experience). Images were contrast adjusted for providing input to the training models (►**Fig. 2**).

Development of the System

A total of 13,845 slices from 37 scans were chosen for the segmentation of the left and right psoas muscles. These slices were then input into the TransUNet-based DLM, as illustrated in ►**Fig. 2**. The U-net, a well-established machine learning algorithm, was employed for segmenting both normal anatomical structures and pathological lesions on medical images.[12] The loss function encompassed a combination of binary cross-entropy and dice loss.[13] The network underwent training for up to 200 epochs, where 60% of the images featured psoas muscles, while the remaining 40% did not. These images were shuffled and paired with their corresponding binary masks, and 80% of these pairs were allocated for training purposes. The training process involved presenting images and their manually segmented muscle counterparts to the algorithm. The deep learning system was educated through datasets containing manually segmented muscles at the L2–L4 levels. Using the manually segmented muscles as the ground truth, the tool's intersection of union was computed for validation purposes.

Testing and HUAC Computation

During the testing phase, the trained model was implemented to perform muscle segmentations at the L2–L4 levels across the remaining 440 slices from the dataset, encompassing the psoas muscle, within the four CT volumes.

Computation of HUAC

To calculate the HUAC score, we resized the input test image as well as its corresponding predicted binary mask to 512×512 pixels. The individual areas (in cm2) of the two psoas muscles were computed using the DLM output, that is, the predicted binary mask. Additionally, the left and right psoas muscles were isolated from the corresponding CT scans using the predicted binary mask image, allowing for the calculation of their mean Hounsfield unit (HU) values (►**Fig. 3**). The HUAC score was then computed based on the formulation shown in ►**Fig. 4**, incorporating the mean HU values and the areas of the left and right psoas muscles.

Training and Validation

The loss and intersection over union (IoU) curves that were obtained during training and validation are shown in ►**Figs. 5** and **6**, respectively.

$$HUAC(left) = \frac{(Area\ of\ left\ psoas) \times (mean\ HU\ of\ left\ psoas)}{Total\ of\ left\ and\ right\ psoas\ area}$$

$$HUAC(right) = \frac{(Area\ of\ right\ psoas) \times (mean\ HU\ of\ right\ psoas)}{Total\ of\ left\ and\ right\ psoas\ area}$$

$$HUAC = \frac{HUAC(left) + HUAC(right)}{2}$$

Fig. 4 Formulae used for the Hounsfield unit average calculation.

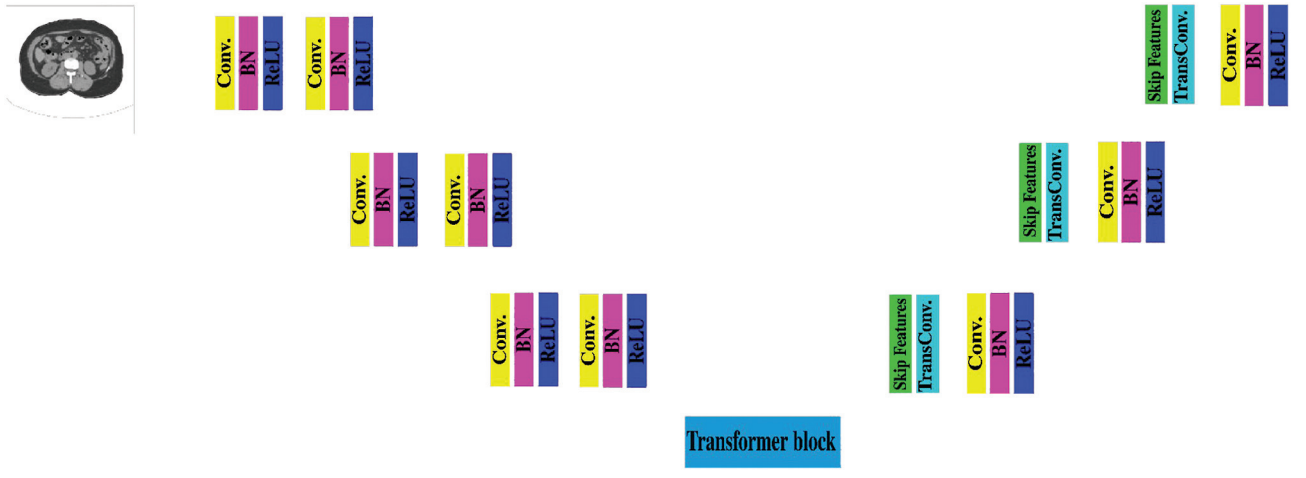

Fig. 3 TransUNet: architectural details. BN, batch normalization; Conv, convolution; RELU, rectified linear unit.

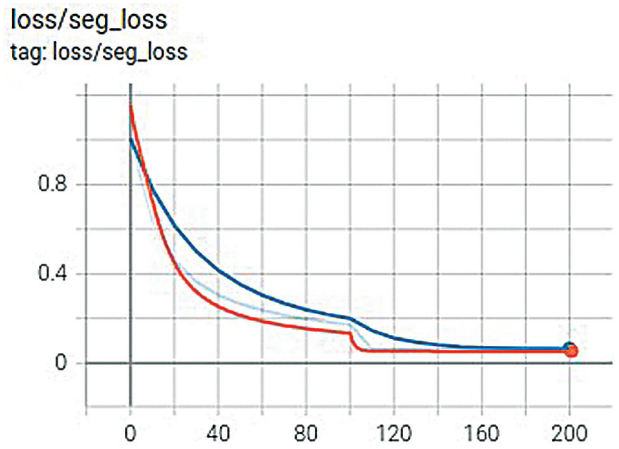

Fig. 5 Loss curves: training and validation. X axis: number of epochs. Y axis: loss.

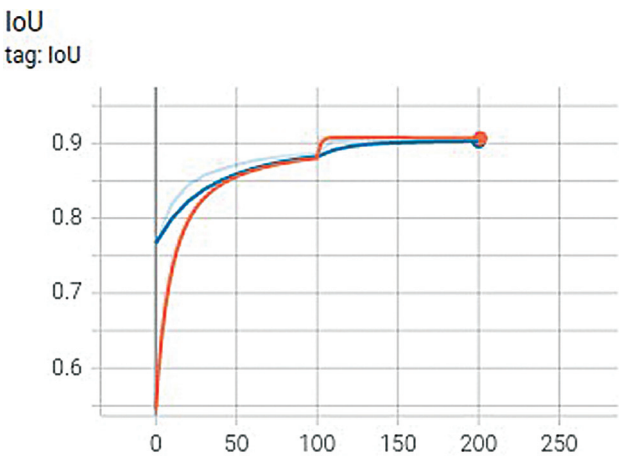

Fig. 6 Intersection over union (IoU) curves: training and validation. X axis: number of epochs. Y axis: IoU.

Results

A test sample is shown in ►**Fig. 7** and the corresponding HUAC computations are shown in ►**Table 1**.

During the inference process, we achieved an average IoU value of 90% and a Dice coefficient of 0.90 when comparing the outputs from the DLM to the corresponding ground truth images. This comparison is depicted in ►**Figs. 8** and **9**. Each point on the curves within the figure corresponds to specific IoU and Dice coefficient values, referring to the ground truth test CT slices.

A few of the 440 test outcomes are illustrated in ►**Fig. 10** showcasing the consistency with their corresponding CTs and the ground truth images.

Discussion

In this study, we introduce our TransUNet-based model designed for the automated segmentation of muscles in CT scans. Our aim is to investigate its precision and accuracy in measuring the HUAC of the psoas muscles and in diagnosing sarcopenia. Notably, our approach involves a novel method to quantify a specific muscle, developed while training on a more compact dataset, as compared with other models.

Our system demonstrates robustness with IoU values surpassing 90% on validation datasets, with an average IoU value of 87% when comparing the DLM output to manually annotated images within the training dataset. The efficiency of this system encompasses variations in CT scanners and image acquisition protocols, as our data originate from two distinct institutions and were collected retrospectively without a firm imaging protocol in place.

Furthermore, our study reveals a Dice coefficient of 0.90 and an average IoU of 0.90. This performance mirrors that of other researchers who have achieved similarly acceptable results in the automated segmentation of abdominal muscles and fat.[14–19] For instance, Lee et al demonstrated a Dice similarity coefficient (DSC) of 0.93 for abdominal muscles,[14] while Weston et al presented a DSC of 0.96 for muscles and 0.94 for visceral fat.[17] It is worth noting that the larger sample size in their training data may contribute to the enhanced outcomes observed in their respective systems.

Sarcopenia is characterized by degenerative skeletal muscle mass loss and has been used as a predictive marker for

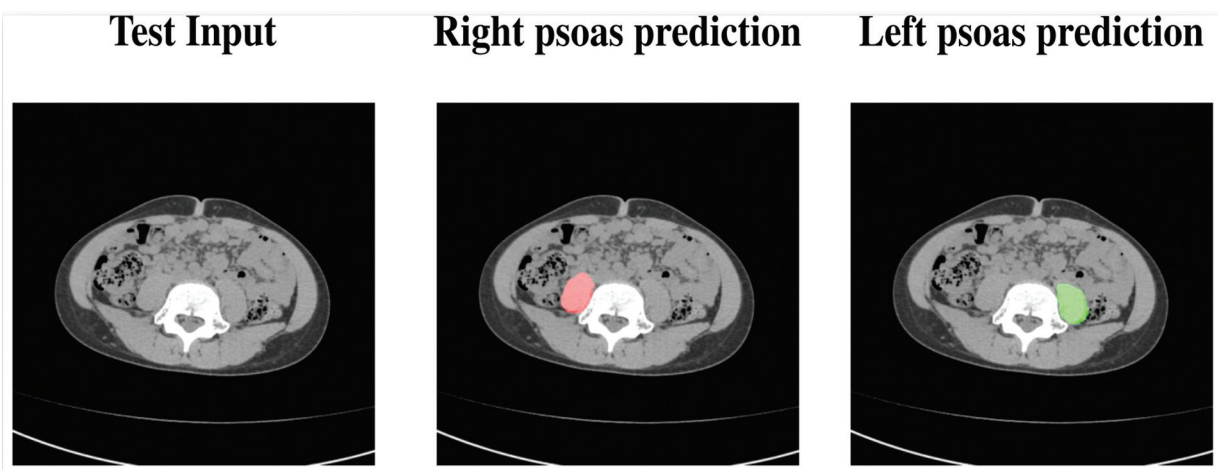

Fig. 7 Input computed tomography with left and right psoas prediction.

Table 1 HUAC computation using the left and right psoas prediction as shown in ►**Fig. 6**

Metrics	Scores
Right psoas area	19.9000
Left psoas area	19.1800
$HUAC_{Right}$	25.7935
$HUAC_{Left}$	21.4721
HUAC	23.6328

Abbreviation: HUAC, Hounsfield unit average calculation.

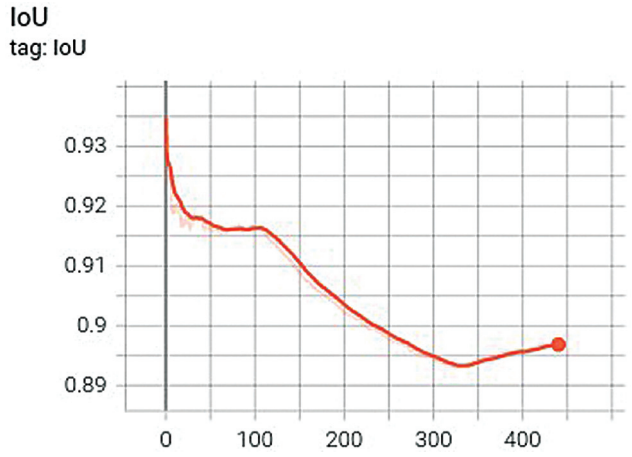

Fig. 8 Intersection over union (IoU) curves at inference. X axis: test slices. Y axis: IoU.

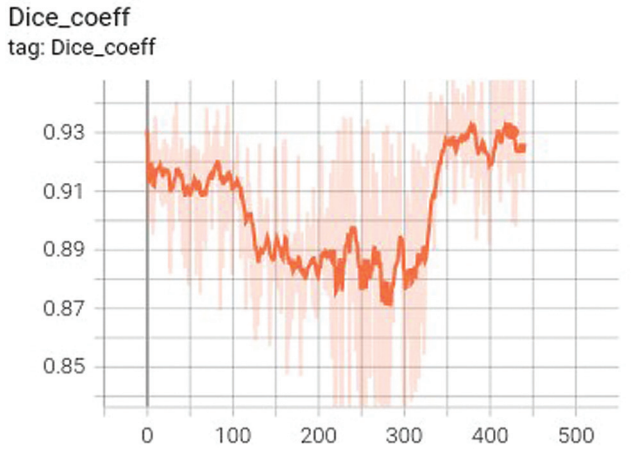

Fig. 9 Dice coefficient at inference. X axis: test slices. Y axis: Dice coefficient.

postoperative complications, driven by its capacity to objectively gauge the patients' nutritional status, fitness, and overall frailty. Several studies underscore its role as a pivotal predictor of morbidity and mortality.[6,20–23] Furthermore, its predictive impact extends beyond mere postoperative adverse events and lends itself to predicting cancer-specific outcomes after hepatic resections, colectomy, and pancreaticoduodenectomies,[24–27] even in patients receiving multimodal therapy.[28,29] Cross-sectional imaging to measure psoas area and density appears to be an effective method to quantify sarcopenia.[30]

Clinical and subjective evaluations of sarcopenia exhibit notable inaccuracies.[31,32] Several modalities, including DEXA and body electrical impedance techniques, have been used to measure it. Even so, CT remains a prominent diagnostic tool and serves as a gold standard for muscle and fat evaluation. Among CT-based muscle mass measurement reports, the L3 level stands as the recommended site, especially for the psoas muscle.[33] This approach exceeds the effectiveness of DEXA scans, particularly in truncal areas.[21] Among comparable indices like Total Psoas Muscle Index, we prefer HUAC due to its broader scope. It encapsulates insights not just related to the psoas expanse but also radiation attenuation, encapsulating both muscle density and fatty infiltration. In our research, we focused on the psoas muscle at the L2–L4 level for HUAC computation.[34,35] The utility of the method extends favorably in obese patients as well. In contrast to segmenting all muscles, isolating only the psoas for surface area and HU assessment has emerged as one of the most predictive factors for adverse postoperative events.[36]

Normally, a solitary axial CT image suffices to gauge muscle cross-sectional area, employing manual or semiautomated tissue segmentation techniques. However, these methods demand considerable time and effort, rendering them impractical for high-volume clinical settings. Several researchers have aimed to employ automated computer systems for truncal musculature quantification. The integration of deep learning algorithms has substantially diminished interobserver variability, furnishing an accurate and replicable sarcopenia evaluation.

Sarcopenia assessment serves not merely as a patient stratification tool but also to guide focused interventions toward those who require them most. Nutritionists can tailor diets for surgical patients, while therapists can determine exercise regimen intensities, both of which have demonstrated efficacy in reversing the frailty linked to sarcopenia.[37] Our hypothesis posits that identifying at-risk patients through an automated CT imaging tool, often already a part of their diagnostic process, can significantly enhance not only short-term hospital outcomes but also long-term results following discharge and return home.[38]

Several limitations are inherent in our study. Due to its retrospective nature, patient recruitment lacked a consecutive pattern and may have introduced a selection bias. While our inclusion criteria for CT volumes included patients with diverse pathologies, without specific limitations, the resulting small sample size might not be representative of the broader patient population. Additionally, our validation process relied on datasets from only two institutions. Therefore, we recommend extensive validation of the DLM on a larger scale to enhance the robustness and generalizability of our findings.

In conclusion, our study demonstrates the precision of our deep learning algorithm in quantifying the psoas muscle's HUAC, a pivotal marker for sarcopenia. We also

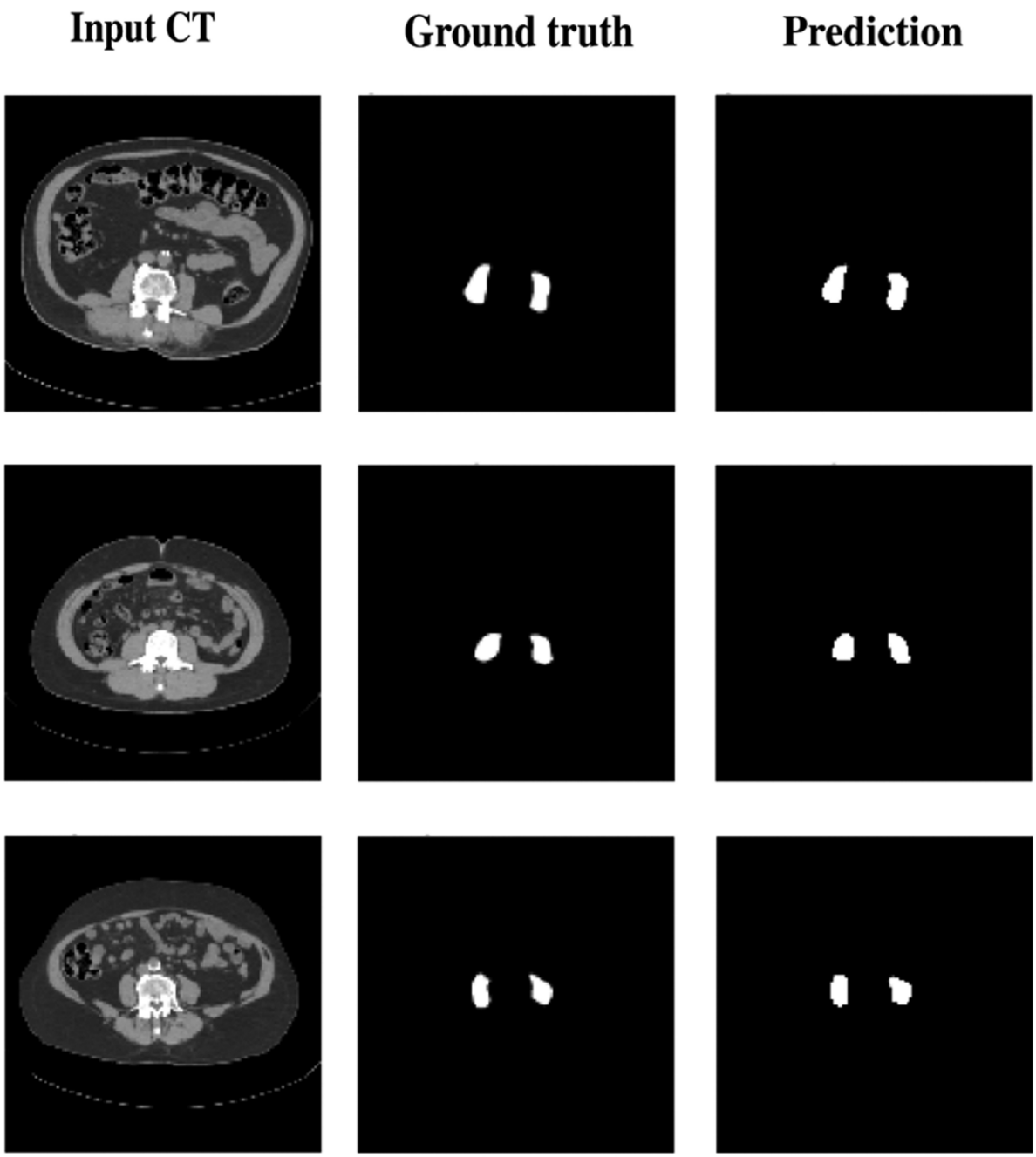

Fig. 10 Input computed tomography scans, ground truth images, and the model predictions at inference.

validate the feasibility of training a neural network effectively with a compact dataset for muscle segmentation. The evolving capabilities of deep learning in pattern recognition, when coupled with methods for accurate L2–L4 slice localization, pave the way for a comprehensive automated HUAC in CT scans. Our findings underscore technology's potential to refine sarcopenia assessment. By integrating deep learning with complementary methods, a streamlined, standardized approach for evaluating muscle health emerges, equipping medical professionals with enhanced diagnostic tools.

Funding
None.

Conflict of Interest
None declared.

References

1 Cruz-Jentoft AJ, Bahat G, Bauer J, et al; Writing Group for the European Working Group on Sarcopenia in Older People 2 (EWGSOP2), and the Extended Group for EWGSOP2. Sarcopenia: revised European consensus on definition and diagnosis. Age Ageing 2019;48(01):16–31

2 Landi F, Liperoti R, Russo A, et al. Sarcopenia as a risk factor for falls in elderly individuals: results from the ilSIRENTE study. Clin Nutr 2012;31(05):652–658
3 Richards SJG, Senadeera SC, Frizelle FA. Sarcopenia, as assessed by psoas cross-sectional area, is predictive of adverse postoperative outcomes in patients undergoing colorectal cancer surgery. Dis Colon Rectum 2020;63(06):807–815
4 `Gariballa S, Alessa A. Sarcopenia: prevalence and prognostic significance in hospitalized patients. Clin Nutr 2013;32(05):772–776
5 Xu J, Wan CS, Ktoris K, Reijnierse EM, Maier AB. Sarcopenia is associated with mortality in adults: a systematic review and meta-analysis. Gerontology 2022;68(04):361–376
6 Boutin RD, Yao L, Canter RJ, Lenchik L. Sarcopenia: current concepts and imaging implications. AJR Am J Roentgenol 2015; 205(03):W255-66
7 Cao L, Chen S, Zou C, et al. A pilot study of the SARC-F scale on screening sarcopenia and physical disability in the Chinese older people. J Nutr Health Aging 2014;18(03):277–283
8 Cao Q, Xiong Y, Zhong Z, Ye Q. Computed tomography-assessed sarcopenia indexes predict major complications following surgery for hepatopancreatobiliary malignancy: a meta-analysis. Ann Nutr Metab 2019;74(01):24–34
9 Wagner D, Marsoner K, Tomberger A, et al. Low skeletal muscle mass outperforms the Charlson Comorbidity Index in risk prediction in patients undergoing pancreatic resections. Eur J Surg Oncol 2018;44(05):658–663
10 National Ethical Guidelines for Biomedical and Health Research Involving Human Participants. 2017. Accessed June 26, 2018 at: https://www.icmr.nic.in/guidelines/ICMR_Ethical_Guidelines_2017.pdf
11 Yushkevich PA, Piven J, Hazlett HC, et al. User-guided 3D active contour segmentation of anatomical structures: significantly improved efficiency and reliability. Neuroimage 2006;31(03): 1116–1128
12 Ronneberger O, Fischer P, Brox T. U-Net: convolutional networks for biomedical image segmentation. In: Navab N, Hornegger J, Wells WM, Frangi AF, eds. Medical Image Computing and Computer-Assisted Intervention – MICCAI 2015. Cham: Springer International Publishing; 2015:234–241
13 Milletari F, Navab N, Ahmadi SA. V-Net: Fully Convolutional Neural Networks for Volumetric Medical Image Segmentation. Paper presented at: 2016 Fourth International Conference on 3D Vision (3DV); October 25–28, 2016; Stanford, CA
14 Lee H, Troschel FM, Tajmir S, et al. Pixel-level deep segmentation: artificial intelligence quantifies muscle on computed tomography for body morphometric analysis. J Digit Imaging 2017;30(04):487–498
15 Burns JE, Yao J, Chalhoub D, Chen JJ, Summers RM. A machine learning algorithm to estimate sarcopenia on abdominal CT. Acad Radiol 2020;27(03):311–320
16 Decazes P, Tonnelet D, Vera P, Gardin I. Anthropometer3D: automatic multi-slice segmentation software for the measurement of anthropometric parameters from CT of PET/CT. J Digit Imaging 2019;32(02):241–250
17 Weston AD, Korfiatis P, Kline TL, et al. Automated abdominal segmentation of CT scans for body composition analysis using deep learning. Radiology 2019;290(03):669–679
18 Bridge CP, Rosenthal M, Wright B, et al. Fully-automated analysis of body composition from CT in cancer patients using convolutional neural networks. In: Stoyanov D, Taylor Z, Sarikaya D, et al, eds. OR 2.0 Context-Aware Operating Theaters, Computer Assisted Robotic Endoscopy, Clinical Image-Based Procedures, and Skin Image Analysis. Cham: Springer; 2018:204–213
19 Popuri K, Cobzas D, Esfandiari N, Baracos V, Jägersand M. Body composition assessment in axial CT images using FEM-based automatic segmentation of skeletal muscle. IEEE Trans Med Imaging 2016;35(02):512–520
20 Onishi S, Tajika M, Tanaka T, et al. Prognostic significance of sarcopenia in patients with unresectable advanced esophageal cancer. J Clin Med 2019;8(10):1647
21 Lee K, Shin Y, Huh J, et al. Recent issues on body composition imaging for sarcopenia evaluation. Korean J Radiol 2019;20(02):205–217
22 Pinto Dos Santos D, Kloeckner R, Koch S, et al. Sarcopenia as prognostic factor for survival after orthotopic liver transplantation. Eur J Gastroenterol Hepatol 2020;32(05):626–634
23 McLean RR, Shardell MD, Alley DE, et al. Criteria for clinically relevant weakness and low lean mass and their longitudinal association with incident mobility impairment and mortality: the foundation for the National Institutes of Health (FNIH) sarcopenia project. J Gerontol A Biol Sci Med Sci 2014;69(05):576–583
24 Peng PD, van Vledder MG, Tsai S, et al. Sarcopenia negatively impacts short-term outcomes in patients undergoing hepatic resection for colorectal liver metastasis. HPB (Oxford) 2011;13 (07):439–446
25 Itoh S, Shirabe K, Matsumoto Y, et al. Effect of body composition on outcomes after hepatic resection for hepatocellular carcinoma. Ann Surg Oncol 2014;21(09):3063–3068
26 Reisinger KW, van Vugt JLA, Tegels JJW, et al. Functional compromise reflected by sarcopenia, frailty, and nutritional depletion predicts adverse postoperative outcome after colorectal cancer surgery. Ann Surg 2015;261(02):345–352
27 Peng P, Hyder O, Firoozmand A, et al. Impact of sarcopenia on outcomes following resection of pancreatic adenocarcinoma. J Gastrointest Surg 2012;16(08):1478–1486
28 Antoun S, Birdsell L, Sawyer MB, Venner P, Escudier B, Baracos VE. Association of skeletal muscle wasting with treatment with sorafenib in patients with advanced renal cell carcinoma: results from a placebo-controlled study. J Clin Oncol 2010;28(06):1054–1060
29 Dodson RM, Firoozmand A, Hyder O, et al. Impact of sarcopenia on outcomes following intra-arterial therapy of hepatic malignancies. J Gastrointest Surg 2013;17(12):2123–2132
30 Kim TN, Choi KM. Sarcopenia: definition, epidemiology, and pathophysiology. J Bone Metab 2013;20(01):1–10
31 Price KL, Earthman CP. Update on body composition tools in clinical settings: computed tomography, ultrasound, and bioimpedance applications for assessment and monitoring. Eur J Clin Nutr 2019;73(02):187–193
32 Sheean PM, Peterson SJ, Gomez Perez S, et al. The prevalence of sarcopenia in patients with respiratory failure classified as normally nourished using computed tomography and subjective global assessment. JPEN J Parenter Enteral Nutr 2014;38(07):873–879
33 Lenchik L, Boutin RD. Sarcopenia: beyond muscle atrophy and into the new frontiers of opportunistic imaging, precision medicine, and machine learning. Semin Musculoskelet Radiol 2018;22 (03):307–322
34 Miller AL, Min LC, Diehl KM, et al. Analytic morphomics corresponds to functional status in older patients. J Surg Res 2014;192(01):19–26
35 Zarinsefat A, Terjimanian MN, Sheetz KH, et al. Perioperative changes in trunk musculature and postoperative outcomes. J Surg Res 2014;191(01):106–112
36 Boutin R, Katz J, Chaudhari A, et al. Significance of sarcopenia in soft-tissue sarcoma patients: do skeletal muscle and fat measures of body composition on routine ct exams help predict clinical outcomes? Paper presented at: Radiological Society of North America 2014 Scientific Assembly and Annual Meeting; November 30 to December 5, 2014; Chicago, IL
37 Ng TP, Feng L, Nyunt MSZ, et al. Nutritional, physical, cognitive, and combination interventions and frailty reversal among older adults: a randomized controlled trial. Am J Med 2015;128(11): 1225–1236.e1
38 Casey CM, Parker EM, Winkler G, Liu X, Lambert GH, Eckstrom E. Lessons learned from implementing CDC's STEADI falls prevention algorithm in primary care. Gerontologist 2017;57(04):787–796